Electroweak corrections to Higgs-strahlung off W/Z bosons at the Tevatron and the LHC with Hawk

Denner, Ansgar ; Dittmaier, Stefan ; Kallweit, Stefan ; Mück, Alexander

Abstract: The associate production of Higgs bosons with W or Z bosons, known as Higgs-strahlung, is an important search channel for Higgs bosons at the hadron colliders Tevatron and LHC for low Higgs-boson masses. We refine a previous calculation of next-to-leading-order electroweak corrections (and recalculate the QCD corrections) upon including the leptonic decay of the W/Z bosons, thereby keeping the fully differential information of the 2-lepton + Higgs final state. The gauge invariance of the W/Z-resonance treatment is ensured by the use of the complex-mass scheme. The electroweak corrections, which are at the level of - (5-10)% for total cross sections, further increase in size with increasing transverse momenta p T in differential cross sections. For instance, for p T,H $\mathop{>}_{raise0.3emsmashriptscriptstylethicksim}$ $200GeV, which is the interesting range at the LHC, the electroweak corrections to WH production reach about -14\% for MH = 120GeV. The described corrections are implemented in the HawkMonteCarlo program, which was initially de boson-fusion channel, and are discussed for various distributions in the production channels textpp/textpoverline textptot l\nu ll^-l^+/+X$.

DOI: https://doi.org/10.1007/JHEP03(2012)075

FR-PHENO-2011-025
PSI-PR-11-04
ZU-TH 29/11
TTK-11-61

Electroweak corrections to Higgs-strahlung off W/Z bosons at the Tevatron and the LHC with HAWK

ANSGAR DENNER[1], STEFAN DITTMAIER[2], STEFAN KALLWEIT[3,4], AND ALEXANDER MÜCK[5]

[1] *Universität Würzburg, Institut für Theoretische Physik und Astrophysik, D-97074 Würzburg, Germany*

[2] *Albert-Ludwigs-Universität Freiburg, Physikalisches Institut, D-79104 Freiburg, Germany*

[3] *Paul Scherrer Institut, Würenlingen und Villigen, CH-5232 Villigen PSI, Switzerland*

[4] *Institut für Theoretische Physik, Universität Zürich, CH-8057 Zürich, Switzerland*

[5] *Institut für Theoretische Teilchenphysik und Kosmologie, RWTH Aachen University, D-52056 Aachen, Germany*

Abstract:

The associate production of Higgs bosons with W or Z bosons, known as Higgs-strahlung, is an important search channel for Higgs bosons at the hadron colliders Tevatron and LHC for low Higgs-boson masses. We refine a previous calculation of next-to-leading-order electroweak corrections (and recalculate the QCD corrections) upon including the leptonic decay of the W/Z bosons, thereby keeping the fully differential information of the 2-lepton + Higgs final state. The gauge invariance of the W/Z-resonance treatment is ensured by the use of the complex-mass scheme. The electroweak corrections, which are at the level of $-(5-10)\%$ for total cross sections, further increase in size with increasing transverse momenta p_{T} in differential cross sections. For instance, for $p_{\mathrm{T,H}} \gtrsim 200\,\mathrm{GeV}$, which is the interesting range at the LHC, the electroweak corrections to WH production reach about -14% for $M_{\mathrm{H}} = 120\,\mathrm{GeV}$. The described corrections are implemented in the HAWK Monte Carlo program, which was initially designed for the vector-boson-fusion channel, and are discussed for various distributions in the production channels $\mathrm{pp/p\bar{p}} \to \mathrm{H} + l\nu_l/l^-l^+/\nu_l\bar{\nu}_l + X$.

December 2011

1 Introduction

The Higgs-strahlung processes at hadron colliders, $\mathrm{pp/p\bar{p}} \to \mathrm{H} + \mathrm{W/Z} \to \mathrm{H} + l\nu_l/l^-l^+/\nu_l\bar{\nu}_l + X$, represent important search channels for a Standard Model (SM) Higgs boson in the low-mass range, which is not only favoured by electroweak precision tests, but also by recent results from Higgs searches at the LHC [1]. At the Tevatron the sensitivity to a light SM Higgs boson almost exclusively results from these channels, and the analysis of the full Tevatron data set might be able to exclude values of the Higgs-boson mass M_H close to the LEP exclusion limit of $M_\mathrm{H} = 114\,\mathrm{GeV}$ beyond the 95% confidence level. At the LHC this low-mass range is explored mainly via inclusive Higgs production employing the $\mathrm{H} \to \gamma\gamma$ decay channel, but Higgs-strahlung slightly improves the sensitivity and provides an interesting additional independent search channel with the Higgs boson decaying via $\mathrm{H} \to \mathrm{b\bar{b}}$. The challenge in all these analyses is background control, both in cross-section normalization and differential distributions. This is particularly pronounced in the boosted $\mathrm{H} + \mathrm{W/Z}$ analysis at the LHC where the $\mathrm{H} \to \mathrm{b\bar{b}}$ decay should be identified from the b-quark substructure within a highly boosted "fat jet" [2].

The mentioned analyses call for precise theoretical predictions with proper estimates of the corresponding theoretical and parametric uncertainties. The next-to-leading-order (NLO) QCD corrections, whose structure is identical to the respective corrections to the Drell–Yan process, were calculated [3] a long time ago and are available, e.g., in the public programs VV2H [4] and MCFM [5]. The most important part of the next-to-next-to-leading-order (NNLO) QCD corrections is similar to the Drell–Yan process as well and was calculated in Ref. [6], using the results of Ref. [7] on the total Drell–Yan cross section. The production of ZH final states additionally receives contributions from gluon fusion via top-quark loops, which was also included in the calculation of Ref. [6]. The remaining NNLO QCD corrections that are not of Drell–Yan type, which involve Higgs couplings to top-quark loops, have been shown to be at the 1−2% level [8]. The calculation of NLO corrections, which are of the order of +30% in QCD, was completed by the NLO electroweak (EW) corrections [9], which turned out to be about −(5−10)%, and a combined prediction for total cross sections at the Tevatron and the LHC was presented in Ref. [10]. An update of the cross-section prediction, together with a thorough estimate of uncertainties, was presented in the first report [11] of the LHC Higgs Cross Section Working Group. For the LHC with a centre-of-mass (CM) energy of 7(14) TeV the QCD scale uncertainties were assessed to be about 1% and 1−2(3−4)% for WH and ZH production, respectively, while uncertainties of the parton distribution functions (PDFs) turn out to be about 3−4%.

These results, however, hold only for total cross sections and have to be generalized to distributions for the experimental analyses, in particular if one employs boosted Higgs bosons. An important step towards differential distributions has been made recently at NNLO QCD in Ref. [12], where the Drell–Yan-like corrections to WH production are calculated while keeping the full kinematical information of the final state.

In this paper we present fully differential NLO EW predictions for the final states $\mathrm{H} + l\nu_l/l^-l^+/\nu_l\bar{\nu}_l + X$, i.e. including the leptonic decays of the W and Z bosons. We also recalculate the corresponding NLO QCD corrections. In contrast to the (N)NLO QCD calculations the EW loop corrections involve also irreducible corrections connecting production and decay of the W/Z bosons. In order to guarantee the gauge invariance of the NLO calculation in spite of the W/Z resonances we employ the complex-mass scheme, which was introduced for leading-order (LO) and NLO calculations in Ref. [13] and Ref. [14], respectively. The use of complex W/Z masses at the same time cures the appearance of perturbative artifacts for Higgs-boson masses near the pair production thresholds at $M_\mathrm{H} = 2M_\mathrm{W}, 2M_\mathrm{Z}$, where the EW corrections to WH/ZH production [9] are singular. The calculation described in this paper will be part of the Monte

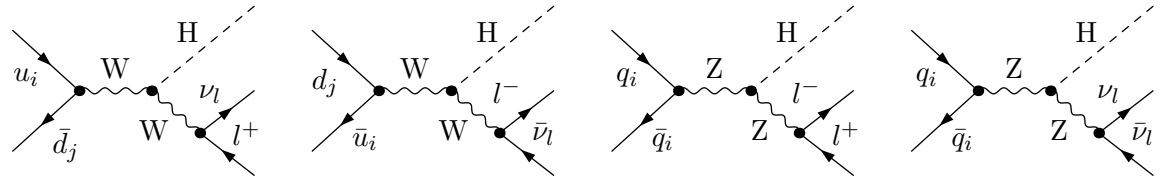

Figure 1: Feynman diagrams for the LO processes (2.1)–(2.4).

Carlo program Hawk, which was originally designed for the description of Higgs production via vector-boson fusion including NLO QCD and EW corrections [15] and is publically available [16].

The paper is organized as follows: In Section 2 we describe the structure of the underlying NLO calculation and the techniques used. Section 3 contains a detailed discussion of numerical results for the processes $\mathrm{pp/p\bar{p}} \to \mathrm{H} + l\nu_l/l^-l^+/\nu_l\bar{\nu}_l + X$ at the Tevatron and the LHC, the latter at CM energies of 7 TeV and 14 TeV. Finally, we conclude in Section 4.

2 Structure of the NLO calculation

2.1 General setup

At LO, the associate production of a Higgs boson H with a weak gauge boson $V = \mathrm{W}, \mathrm{Z}$ can only proceed via quark–antiquark annihilation at hadron colliders. Treating the incoming quarks and the outgoing leptons as massless, the Higgs boson does not couple to the massless fermions, and there is only one LO diagram per channel, see Fig. 1. In detail, the following partonic processes are considered,

$$u_i\,\bar{d}_j \to \mathrm{HW}^+ \to \mathrm{H}\nu_l l^+\,, \tag{2.1}$$
$$d_j\,\bar{u}_i \to \mathrm{HW}^- \to \mathrm{H}l^-\bar{\nu}_l\,, \tag{2.2}$$
$$q_i\,\bar{q}_i \to \mathrm{HZ} \to \mathrm{H}l^-l^+\,, \tag{2.3}$$
$$q_i\,\bar{q}_i \to \mathrm{HZ} \to \mathrm{H}\nu_l\bar{\nu}_l\,, \tag{2.4}$$

where q_i denotes any light quark and u_i, d_i the up- and down-type quarks of the ith generation. The intermediate W/Z-boson resonances are described by complex W/Z-boson masses μ_V via the replacement

$$M_V^2 \to \mu_V^2 = M_V^2 - \mathrm{i}M_V\Gamma_V, \quad V = \mathrm{W}, \mathrm{Z} \tag{2.5}$$

in the V propagator as dictated by the complex-mass scheme (see below). Hence, all our results correspond to a fixed-width description of the Breit–Wigner resonance. Moreover, all related quantities, in particular the weak mixing angle, are formulated in terms of the complex mass parameters.

The final-state leptons are treated as massless unless their small masses are used to regularize a collinear divergence. Concerning bremsstrahlung, we support the possibility that collinear photons may be completely separated from an outgoing charged lepton, because this situation is relevant for muons. More details on the treatment of such non-collinear-safe observables are described below.

The light quarks are considered massless as well, in line with the parton-model requirements. This means that the quark mixing matrix only appears as global weight factor $|V_{ij}|^2$ in the

processes (2.1) and (2.2). Mixing with the third generation is neglected throughout. Owing to the smallness of the $b\bar{b}$ contribution to ZH production, which amounts to approximately 1(3)% at the 7(14) TeV LHC for an inclusive analysis, 0.5(1)% for a boosted analysis, and is negligible at the Tevatron, the $b\bar{b}$ annihilation channels are treated in LO only.

To define the electromagnetic coupling constant α, we use the G_μ scheme, i.e. we derive α from the Fermi constant according to

$$\alpha_{G_\mu} = \frac{\sqrt{2} G_\mu M_\mathrm{W}^2}{\pi} \left(1 - \frac{M_\mathrm{W}^2}{M_\mathrm{Z}^2}\right). \tag{2.6}$$

In this scheme, the weak corrections to muon decay, Δr, are included in the charge renormalization constant (see e.g. Ref. [9]). As a consequence, the EW corrections are independent of logarithms of the light-quark masses. Moreover, this definition effectively resums the contributions associated with the running of α from zero to the weak scale and absorbs some leading universal corrections $\propto G_\mu m_\mathrm{t}^2$ from the ρ parameter into the LO amplitude. For corrections due to collinear final-state radiation it would be more appropriate to use $\alpha(0)$ defined in the Thomson limit to describe the corresponding coupling. On the other hand, using α_{G_μ} everywhere is best suited to describe the larger genuine weak corrections which are present in the Higgs-strahlung processes. Thus, the optimal choice cannot be achieved in one particular input scheme, and the calculation could be refined beyond NLO. Among other things, higher-order effects from multi-photon emission should also be included at this level of precision which is beyond the scope of this work. However, this kind of sophistication will not be needed in practice, since the expected statistics does not allow for this level of accuracy in the experimental analysis either.

The major part of the calculation could be carried over from the calculation of NLO QCD and EW corrections to Higgs + 2 jet production as described in Ref. [15]. In detail, we had to discard the vector-boson fusion contribution (t/u channels) and to keep only the s-channel part from Ref. [15] adjusting the quantum numbers of the final-state fermions, which are leptons for the Higgs-strahlung processes under consideration.

All results are checked against a completely new and independent second calculation based on FeynArts 3.2 [17] and FormCalc 3.1 [18]. The translation of the amplitudes into the Weyl–van-der-Waerden formalism as presented in Ref. [19] is performed with the program Pole [20]. Pole also provides an interface to the multi-channel phase-space integrator Lusifer [21] which has been extended to use Vegas in order to optimize each phase-space mapping. The results of the two calculations are in mutual agreement.

2.2 Virtual corrections

The actual loop calculation, which was also the basis for the loop calculation [15] entering Hawk, goes back to the calculation [22] of NLO QCD and EW corrections to the four-body Higgs decays $\mathrm{H} \to \mathrm{WW/ZZ} \to 4\,\text{fermions}$, where the same amplitudes appear in a crossed variant. We make use of those results, which were obtained in the traditional Feynman-diagrammatic approach and checked against the independent second calculation.

The virtual corrections modify the partonic processes that are already present at LO; there are about 200 one-loop diagrams per tree diagram depending on the channel. At NLO these corrections are induced by self-energy, vertex, box (4-point), and pentagon (5-point) diagrams, shown schematically in Fig. 2. For the implementation of the finite W/Z widths the complex-mass scheme is employed, which was introduced in Ref. [13] for LO calculations and generalized to the one-loop level in Ref. [14]. In this approach the W- and Z-boson masses are consistently considered as complex quantities, defined as the locations of the propagator poles in the complex

Self-energy diagrams:

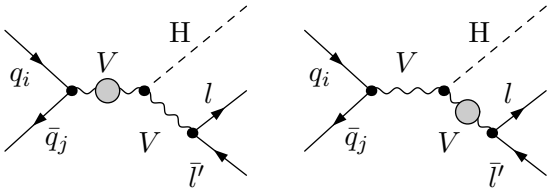

Vertex diagrams:

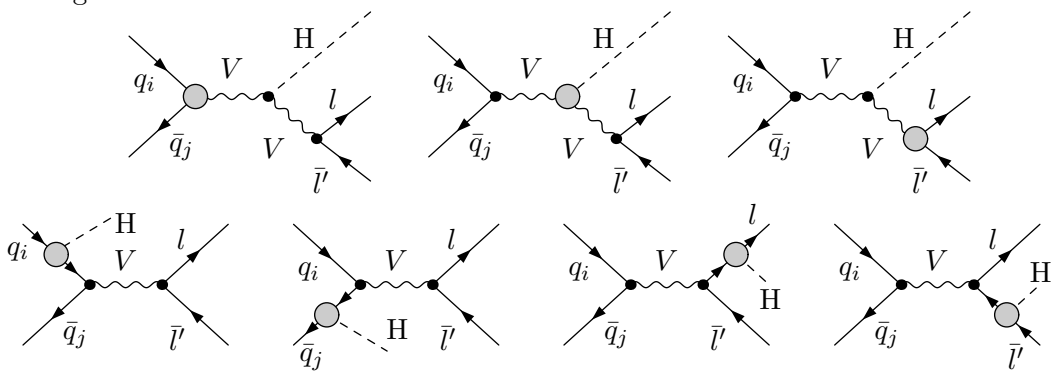

Box and pentagon diagrams:

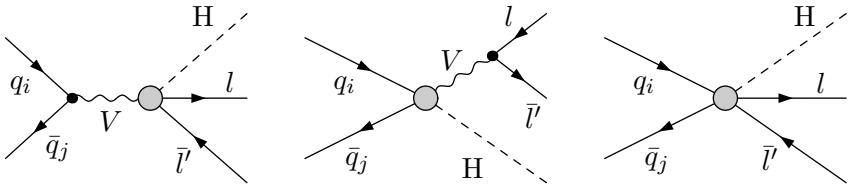

Figure 2: Different classes of loop diagrams with up to 5 external legs corresponding to the virtual corrections to the LO processes (2.1)–(2.4). Note that there are loop-induced vertex diagrams for the coupling of the Higgs boson to the external massless fermions which are absent at tree level.

plane. This leads to complex couplings and, in particular, a complex weak mixing angle. The scheme fully respects all relations that follow from gauge invariance.

The underlying calculation [22] of the $\mathrm{H} \to 4f$ amplitudes was performed both in the conventional 't Hooft–Feynman gauge and in the background-field formalism using the conventions of Refs. [23] and [24], respectively. The amplitudes were generated with FeynArts 1.0 [25] and further manipulated with in-house programs written in *Mathematica*, which automatically create building blocks in *Fortran*. The amplitudes are expressed in terms of standard matrix elements, which contain the fermionic spinor chains, and coefficients, which contain the tensor integrals, couplings, etc. The tensor integrals are recursively reduced to scalar master integrals at the numerical level. Tensor and scalar 5-point functions are directly expressed in terms of 4-point integrals [26, 27]. Tensor 4-point and 3-point integrals are reduced to scalar integrals with the Passarino–Veltman algorithm [28] as long as no small Gram determinant appears in the reduction. If small Gram determinants occur, we expand the tensor coefficients about the limit of vanishing Gram determinants and possibly other kinematical determinants, as described in Ref. [27] in detail. For the evaluation of the scalar integrals with complex masses we use two independent in-house libraries based on the general results listed in Ref. [29].

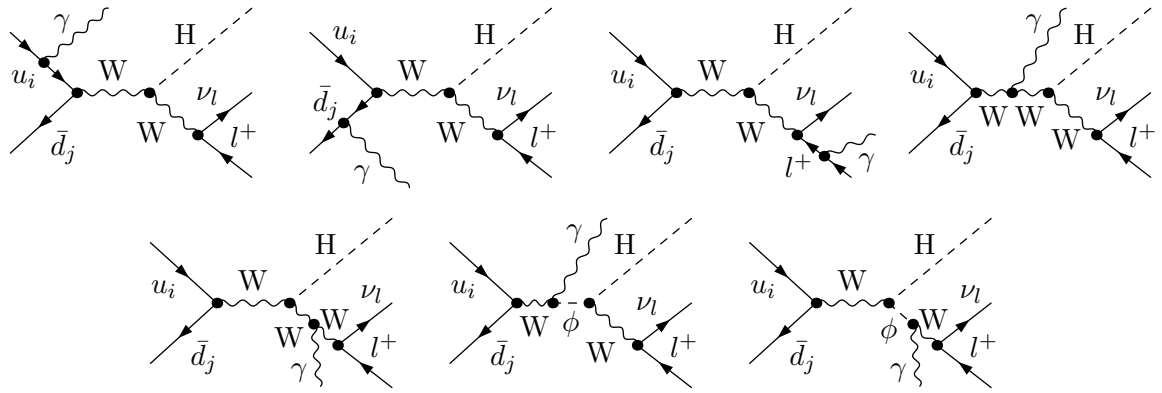

Figure 3: Feynman diagrams for real photonic bremsstrahlung corrections to the LO process (2.1). A photon cannot only be emitted from the external charged fermions, but also from the intermediate W bosons. In Feynman gauge, there are also diagrams involving the charged Goldstone boson ϕ.

2.3 Real corrections

The EW real corrections to the partonic processes (2.1)–(2.4) consist of photon bremsstrahlung,

$$u_i\ \bar{d}_j \to \mathrm{HW}^+ \to \mathrm{H}\nu_l l^+\gamma\,, \tag{2.7}$$

$$d_j\ \bar{u}_i \to \mathrm{HW}^- \to \mathrm{H}l^-\bar{\nu}_l\gamma\,, \tag{2.8}$$

$$q_i\ \bar{q}_i \to \mathrm{HZ} \to \mathrm{H}l^-l^+\gamma\,, \tag{2.9}$$

$$q_i\ \bar{q}_i \to \mathrm{HZ} \to \mathrm{H}\nu_l\bar{\nu}_l\gamma\,, \tag{2.10}$$

with Feynman diagrams shown exemplarily for the process (2.7) in Fig. 3, and of photon-induced processes, which involve the same amplitudes as the bremsstrahlung processes, but with the photon crossed into the initial state in all possible ways. The technical implementation of the real corrections again basically follows along the same lines as in the NLO calculation within HAWK for Higgs + 2 jet production [15, 16], employing dipole subtraction [30–32].

Due to the emission of soft photons the real corrections include soft singularities which are cancelled by the virtual corrections independently of the details of the event selection or recombination procedure. The treatment of left-over collinear singularities related to splittings involving photons and fermions requires particular care:

- *Photonic initial-state radiation*
  The collinear singularities from photonic initial-state radiation off quarks are absorbed by a redefinition of the PDFs similar to the standard factorization procedure in QCD, but employing the DIS scheme. At present, the PDF set MRSTQED2004 [33] is the only one that takes into account $\mathcal{O}(\alpha)$ corrections. However, applications with this PDF set and older estimate of $\mathcal{O}(\alpha)$ effects on PDFs show that the impact of these PDF corrections is at most at the per-cent level [34]. For the time being, it is, thus, advisable to use an up-to-date PDF set that ignores $\mathcal{O}(\alpha)$ corrections, but includes recent improvements on the QCD side, because the latter have an impact on PDFs much larger than 1%.

- *Photon-induced processes, $\gamma \to q\bar{q}^*/\bar{q}q^*$ splitting*
  In the photon-induced processes, the collinear singularities resulting from the splittings

$\gamma \to q\bar{q}^*/\bar{q}q^*$ are removed in the process of PDF redefinitions as well. Moreover, the evaluation of the photon-induced channels requires a photon distribution function and its inclusion in the PDF evolution. Using the MRSTQED2004 PDF set for this task is certainly legitimate, since the contribution from initial-state photons is comparably small.

- *Collinear final-state radiation*
  Next, we consider collinear final-state radiation off leptons. If collinear photons and charged leptons are recombined into a pseudo-particle (mimicking the start of hadronic or electromagnetic showers) to form IR-safe observables, all the remaining singularities arising from collinear photon emission in the final state also cancel against the corresponding singularities in the virtual corrections. For muons in the final state, however, it is experimentally possible to separate collinear photons from the lepton, i.e. to observe so-called "bare" muons. Hence, the resulting cross sections are not collinear safe (i.e. the KLN theorem [35] does not apply), and the corresponding collinear singularities show up as logarithms of the small lepton (muon) mass. The lepton mass cuts off the collinear divergence in a physically meaningful way. We employ the extension [32] of the subtraction formalism [30, 31], which allows for calculating cross sections for bare leptons, i.e. cross sections defined without any photon recombination. Like in the standard subtraction formalism, it is sufficient to calculate the real-emission matrix elements for the partonic processes in the massless-fermion approximation. The main difference between the subtraction variants of Refs. [31] and [32] concerns the implementation of phase-space cuts. In the standard subtraction formalism [31] it is always assumed that the complete momentum of the lepton and a collinear photon is subject to cuts (as it would be the case after recombination), while the generalization [32] allows for non-collinear-safe cuts that resolve the distribution of the momenta in collinear photon–lepton configurations. This more general cut procedure in the non-collinear-safe case has to be carefully implemented both in the real-emission part and the corresponding subtraction terms, in order to ensure the numerical cancellation of singularities. Of course, the treatment of non-collinear-safe cuts leads to a modification of the re-added subtraction part as well. In the formulation of Ref. [32] this modification assumes the form of an additional (+)-distribution which contains the surviving mass singularity. This (+)-distribution integrates to zero for collinear-safe observables so that the formalism reduces to the well-known standard subtraction formalism. For non-collinear-safe observables the additional logarithms of the lepton mass in the final result are, thus, isolated analytically. For a complete and detailed description of this more general subtraction formalism we refer the reader to Ref. [32].

- *Photon-induced processes, $\gamma \to l\bar{l}^*/\bar{l}l^*$ splitting*
  Finally, there are also collinear configurations connected with the splittings $\gamma \to l\bar{l}^*/\bar{l}l^*$ if charged leptons are allowed to escape into the beam pipe. For instance, in our numerical analysis in Section 3, we also provide predictions for a contribution to the $\mathrm{H} + \nu_l\bar{\nu}_l$ channels which stems from WH production, where the charged lepton is not identified in the detector. While the EW corrections are conceptually not different for the quark-induced processes, the photon-induced processes have to be treated carefully, in particular the contribution where the incoming photon is splitting into a charged lepton pair, which leads to an enhancement by a logarithm in the lepton mass. The subtraction formalism to extract these logarithms analytically is available [32] and proceeds as for the photonic splitting into quarks. However, in contrast to the splitting into quarks the mass logarithm is not absorbed into the definition of the PDF (there is no lepton PDF), but is part of the re-

sult. For the numerics in Section 3, we use the mass of the electron in this logarithmically enhanced term.

3 Numerical results

3.1 Input parameters and setup

For the numerical evaluation we adopt the input parameters used by the LHC Higgs Cross Section Working Group in Ref. [11],

$$\begin{aligned}
G_\mu &= 1.16637 \times 10^{-5}\,\text{GeV}^{-2}, \quad & \alpha_\text{s}(M_\text{Z})|_\text{NLO} &= 0.1202, & & \\
M_\text{W}^\text{OS} &= 80.398\,\text{GeV}, & \Gamma_\text{W}^\text{OS} &= 2.0887\,\text{GeV}, & & \\
M_\text{Z}^\text{OS} &= 91.1876\,\text{GeV}, & \Gamma_\text{Z}^\text{OS} &= 2.4952\,\text{GeV}, & M_\text{H} &= 120\,\text{GeV}, \\
m_\text{e} &= 0.510998910\,\text{MeV}, & m_\mu &= 105.658367\,\text{MeV}, & m_\text{t} &= 172.5\,\text{GeV}, \\
|V_\text{ud}| &= |V_\text{cs}| = 0.974, & |V_\text{us}| &= |V_\text{cd}| = \sqrt{1-|V_\text{cs}|^2}, & &
\end{aligned} \tag{3.1}$$

which essentially follow Ref. [36]. Note that we use the measured width $\Gamma_\text{Z}^\text{OS}$ for the Z boson, but the calculated on-shell width $\Gamma_\text{W}^\text{OS}$ for the W boson as input. The CKM matrix is included via global factors in the partonic cross sections for the different possible quark flavours. The small mixing between the first two and the third generation is neglected. Within loops the CKM matrix is set to unity, because its effect is negligible there.

Using the complex-mass scheme [14], we employ a fixed width in the resonant W- and Z-boson propagators in contrast to the approach used at LEP and Tevatron to fit the W and Z resonances, where running widths are taken. Therefore, we have to convert the "on-shell" (OS) values of M_V^OS and Γ_V^OS ($V = \text{W}, \text{Z}$), resulting from LEP and Tevatron, to the "pole values" denoted by M_V and Γ_V. The relation between the two sets of values is given by [37]

$$M_V = M_V^\text{OS}/\sqrt{1+(\Gamma_V^\text{OS}/M_V^\text{OS})^2}, \qquad \Gamma_V = \Gamma_V^\text{OS}/\sqrt{1+(\Gamma_V^\text{OS}/M_V^\text{OS})^2}, \tag{3.2}$$

leading to

$$\begin{aligned}
M_\text{W} &= 80.370\ldots\,\text{GeV}, \qquad \Gamma_\text{W} = 2.0880\ldots\,\text{GeV}, \\
M_\text{Z} &= 91.153\ldots\,\text{GeV}, \qquad \Gamma_\text{Z} = 2.4943\ldots\,\text{GeV}.
\end{aligned} \tag{3.3}$$

We make use of these mass and width parameters in the numerics discussed below, although the difference between using M_V or M_V^OS would be hardly visible.

As explained in Section 2.1, we adopt the G_μ scheme, where the electromagnetic coupling α is set to α_{G_μ} (2.6). In this scheme the electric-charge renormalization constant does not contain logarithms of the light-fermion masses, in contrast to the $\alpha(0)$ scheme, so that the results become practically independent of the light-quark masses.

The MSTW2008NLO/LO PDF set [38] is used throughout implying the values of $\alpha_\text{s}(M_\text{Z})$ stated in (3.1) at NLO. We use standard running of the strong coupling constant as provided by the LHAPDF implementation of the PDF sets [39]. Only the photon-induced processes are evaluated with the MRSTQED2004 set of PDFs [33]. The QCD and QED factorization scales as well as the renormalization scale are always identified and set to

$$\mu = M_V + M_\text{H}\,. \tag{3.4}$$

For a study of the scale and PDF uncertainties in Higgs-strahlung processes, we refer the reader to the report of the LHC Higgs Cross Section Working Group [11] for total cross sections and to the upcoming second report [40] on differential distributions.

In the following, we present results for the Tevatron at a CM energy of $\sqrt{s} = 1.96\,\text{TeV}$ and for the LHC with $\sqrt{s} = 7\,\text{TeV}$ and $14\,\text{TeV}$.

3.2 Phase-space cuts and event selection

Since WH and ZH production with leptonically decaying W and Z bosons do not involve outgoing QCD partons in LO, there is at most one QCD parton in the final state in our fixed-order NLO predictions, so that no jet algorithm has to be applied.

As explained above, we alternatively apply two versions of handling photons that can become collinear to outgoing charged leptons. The first option is to assume a perfect isolation between charged leptons and photons, an assumption that is at least approximately fulfilled for (bare) muons. The second option performs a recombination of photons and nearly collinear charged leptons and, thus, mimics the inclusive treatment of electrons within electromagnetic showers in the detector. Specifically, a photon γ and a lepton l are recombined for $R_{\gamma l} < 0.1$, where $R_{\gamma l} = \sqrt{(y_l - y_\gamma)^2 + \phi_{l\gamma}^2}$ is the usual separation variable in the y–ϕ-plane with y denoting the rapidity and $\phi_{l\gamma}$ the angle between l and γ in the plane perpendicular to the beams. If l and γ are recombined, we simply add their four-momenta and treat the resulting object as a quasi-lepton. If more than one charged lepton is present in the final state, the possible recombination is performed with the lepton delivering the smaller value of $R_{\gamma l}$.

After applying the recombination procedure we impose the following cuts on the charged leptons,

$$p_{\text{T},l} > 20\,\text{GeV}, \qquad |y_l| < 2.5, \tag{3.5}$$

where $p_{\text{T},l}$ is the transverse momentum of lepton l. For channels with at least one neutrino in the final state we require a missing transverse momentum

$$\not{p}_\text{T} > 25\,\text{GeV}\,, \tag{3.6}$$

which is equal to the total transverse momentum of the neutrinos in the events. While the two-body decay of the Higgs boson is implemented in HAWK, in this work we do not employ identification cuts on the decay products of the Higgs boson.

For the LHC, we also discuss the impact of the optional additional cuts

$$p_{\text{T,H}} > 200\,\text{GeV}, \qquad p_{\text{T,W/Z}} > 190\,\text{GeV} \tag{3.7}$$

on the transverse momentum of the Higgs and the weak gauge boson, respectively. The corresponding selection of events with boosted Higgs bosons is improving the signal-to-background ratio in the context of employing the measurement of the jet substructure in $\text{H} \to \text{b}\bar{\text{b}}$ decays leading to a single fat jet. The need for background suppression calls for (almost) identical cuts on the transverse momentum of the vector bosons and the Higgs boson [41]. However, symmetric cuts induce large radiative corrections in fixed-order calculations in the corresponding p_T distributions near the cut. Since the Higgs boson and the vector boson are back-to-back at LO, any initial-state radiation will either decrease $p_{\text{T,H}}$ or $p_{\text{T,W/Z}}$, and the event may not pass the cut anymore. Hence, the differential cross section near the cut is sensitive to almost collinear and/or rather soft initial-state radiation. By choosing the above (slightly asymmetric) cuts this large sensitivity to higher-order corrections can be removed for the important $p_{\text{T,H}}$-distribution. Of

course, since the LO distribution for $p_{\mathrm{T,W/Z}}$ is vanishing for $p_{\mathrm{T,W/Z}} < 200$ GeV due to the $p_{\mathrm{T,H}}$ cut, the higher-order corrections to the $p_{\mathrm{T,W/Z}}$ distributions are still large in this region.

The channel with a Higgs boson and only missing p_{T} also receives a contribution from WH production where the charged lepton is not identified, which we label $\mathrm{H}\nu_l/\overline{\nu}_l$. In our setup, a lepton is not identified if it fails to pass either the $p_{\mathrm{T},l}$ or the y_l cut in (3.5). Following our generic setup, we still consider only the neutrino momentum to calculate $\not{p}_{\mathrm{T}}$. Since in this case $\not{p}_{\mathrm{T}}$ and $p_{\mathrm{T,W}}$ are indistinguishable, we also discard the momentum of the charged lepton when calculating the transverse momentum of the vector boson, i.e. we set $p_{\mathrm{T},V} = \not{p}_{\mathrm{T}}$ in this particular case.

3.3 Results for the LHC and the Tevatron

In this section, we present numerical results for (differential) cross sections and various corrections to the Higgs-production channels with one charged lepton and missing transverse momentum ($\mathrm{H}l^+\nu_l$ and $\mathrm{H}l^-\overline{\nu}_l$), with two charged leptons ($\mathrm{H}l^+l^-$), and with missing momentum only in the final state. For the latter, we distinguish the Z-mediated process ($\mathrm{H}\nu_l\overline{\nu}_l$) and the W-mediated ($\mathrm{H}\nu_l/\overline{\nu}_l$) process, where the charged lepton is not measured in the detector. Of course, the two sources are not distinguishable experimentally. However, since the contribution of the two sources varies considerably with the applied identification cuts, we state the results separately. For the $\mathrm{H}\nu_l/\overline{\nu}_l$ channel we simply invert the identification cuts (3.5) for the charged lepton (see discussion at the end of Section 3.2) while all other cuts and the recombination procedure is applied without changes (see Section 2.3 for subtleties concerning the photon-induced processes). Thus, the resulting cross section may serve as an upper bound on the contribution to the channel with a Higgs boson and only missing transverse momentum in the experimental analysis.

Concerning the EW corrections, we distinguish bare muons and final states with lepton–photon recombination, as introduced in Section 3.2. The corresponding corrections are labelled $\delta_{\mathrm{EW}}^{\mathrm{bare}}$ and $\delta_{\mathrm{EW}}^{\mathrm{rec}}$, respectively. While the latter is independent of the specific charged lepton in the final state, $\delta_{\mathrm{EW}}^{\mathrm{bare}}$ contains fermion-mass logarithms and depends on the lepton mass which is taken to be the muon mass. The contributions due to photon-induced processes are also given in terms of their relative size with respect to the LO cross section and are labelled δ_γ.

All cross sections are given for a specific leptonic state (e.g. $\mathrm{e}^+\mathrm{e}^-$, $\mu^+\mu^-$, or $\nu_\mu\bar{\nu}_\mu$). While the bare corrections are only applicable for the muon final state, the results with lepton–photon recombination are equally valid for electrons and muons. For the process $\mathrm{H}\nu_l\overline{\nu}_l$, there is of course no recombination to be applied, i.e. $\delta_{\mathrm{EW}}^{\mathrm{rec}} = \delta_{\mathrm{EW}}^{\mathrm{bare}}$, and the results are valid for all three generations. Hence, the total ZH cross section with invisible Z decay can be trivially obtained by multiplying the given result by three. On the other hand, the photon-induced contribution to $\mathrm{H}\nu_l/\overline{\nu}_l$ depends on the fermion generation and we show numerical results for the electron channel. The corrections in the muon and tau channels are smaller since the corresponding logarithms of the fermion masses are smaller.

In a single run HAWK employs a single set of PDFs and produces the following NLO prediction,

$$\sigma_{\mathrm{HAWK}}^{\mathrm{NLO}} = \sigma_0 \times (1 + \delta_{\mathrm{QCD}} + \delta_\gamma + \delta_{\mathrm{EW}})\,. \tag{3.8}$$

Note that the LO part σ_0 is calculated with NLO PDFs in that case, i.e. it is not equal to the proper LO cross section σ^{LO}, which is to be calculated with LO PDFs and requires a separate run of HAWK. Likewise, $(1 + \delta_{\mathrm{QCD}})$ is not equal to the standard QCD K-factor $K_{\mathrm{QCD}} = \sigma_{\mathrm{QCD}}^{\mathrm{NLO}}/\sigma^{\mathrm{LO}}$. In the spirit of factorizing QCD and EW corrections, which is certainly true for corrections that are dominated by soft or collinear gluons, the fixed-NLO prediction (3.8) can be improved by

$$\sigma_{\mathrm{fact}}^{\mathrm{NLO}} = \sigma_{\mathrm{QCD}}^{\mathrm{NLO}} \times (1 + \delta_{\mathrm{EW}}) + \sigma_0\,\delta_\gamma, \qquad \sigma_{\mathrm{QCD}}^{\mathrm{NLO}} = \sigma_0\,(1 + \delta_{\mathrm{QCD}})\,, \tag{3.9}$$

and we show predictions for the electron case, i.e. $\delta_{\rm EW} = \delta_{\rm EW}^{\rm rec}$ in the numerical results below. The NLO EW correction factor $\delta_{\rm EW}$ is rather insensitive to changes in the PDFs, but involves a small dependence on the QED factorization scale. Recall that the presently missing $\mathcal{O}(\alpha)$ corrections to the PDFs induce an uncertainty at the level $\lesssim 1\%$, i.e. for full $\mathcal{O}(\alpha)$ precision QED-improved PDFs are needed. To fix full $\mathcal{O}(\alpha\alpha_{\rm s})$ precision beyond this factorization ansatz, a full two-loop calculation would be required, which would certainly be overkill for the data analyses at the Tevatron and LHC. Equation (3.9) also offers a simple possibility to further improve the NLO result to include the NNLO QCD predictions by other authors [6, 12] upon replacing $\sigma_{\rm QCD}^{\rm NLO}$ by $\sigma_{\rm QCD}^{\rm NNLO}$. For WH production this is done in Ref. [40], where our results for $\delta_{\rm EW}$ are used.

In Figure 4 we show our best predictions $\sigma_{\rm fact}^{\rm NLO}$ for the cross section and the EW corrections for the five Higgs-production channels under consideration. We show the results for the inclusive analysis at the Tevatron as well as for the boosted analysis at the LHC running at a CM energy of 7 TeV. As expected, the EW corrections become more and more negative with rising CM energy of typical events and, thus, are larger in absolute terms for the boosted analysis. Their size depends on the channel and exceeds -15% for the boosted analysis. As a function of the Higgs-boson mass, the corrections show small dips around $M_{\rm H} = 2M_{\rm W}$ and $M_{\rm H} = 2M_{\rm Z}$ corresponding to threshold singularities of vector-boson pairs inside loops which are automatically regularized by the complex-mass scheme in our calculation. Earlier predictions in Ref. [9] have been singular at these thresholds. Away from these thresholds, the corrections for the inclusive analysis differ, as expected, only at the level of $1-2\%$ from the predictions for total cross sections for on-shell gauge bosons shown in Ref. [9], mainly due to the effect of final-state radiation in the presence of lepton identification cuts. For the inclusive analysis, the cross section of the $\mathrm{H}\nu_l/\overline{\nu}_l$ channel contributes a sizable fraction to the Higgs plus missing transverse momentum cross section. For the boosted analysis, where the vector boson has to possess a large transverse momentum, it is more unlikely for the charged lepton not to be detected and the contribution due to a missed charged lepton is negligible (below 0.1 fb at the 7 TeV LHC).

In Figure 5, we show the EW corrections for $\mathrm{H}l^+\nu_l$ production at the Tevatron and the LHC at 7 and 14 TeV. The differences between the corrections at the colliders are rather small, at the 1% level. As already indicated above, the EW corrections are insensitive to the choice of the PDF set. Note that there is only a small difference of about 1% or 2% between the cases of bare or recombined leptons, where the larger value of 2% refers to the boosted-Higgs analyses. This small difference reflects the fact that the major part of the EW correction is not due to final-state radiation, but due to non-universal weak corrections.

In Figure 6, we show the contribution from photon-induced processes to the W-mediated channels at the LHC. The contribution to the channels, where the charged lepton is identified, is at the $1-2\%$ level for the boosted analysis and mainly results from diagrams where the initial-state photon couples to a t-channel W boson. Accordingly, the corrections are almost zero for the Z-mediated channels (not shown). There are larger photon-induced corrections for WH production, rising to 8%, to the inclusive cross section at the LHC for large Higgs masses around 200 GeV. Moreover, the photon-induced corrections to the $\mathrm{H}\nu_l/\overline{\nu}_l$ channel, which are additionally enhanced by logarithms of the charged lepton mass, for boosted Higgs bosons are larger than 10% (for the photon splitting into an $\mathrm{e}^+\mathrm{e}^-$ pair) of the corresponding LO $\mathrm{H}\nu_l/\overline{\nu}_l$ cross section and even more sizable for the inclusive setup, in particular for high Higgs masses. Whether these large corrections become phenomenologically relevant at the LHC depends on the details of the analysis. At the Tevatron the corresponding corrections do not exceed 3%.

To facilitate a possible comparison of our results with future results of other groups, in Tables 1 and 2, we show the cross sections and corrections for $M_{\rm H} = 120$ GeV.

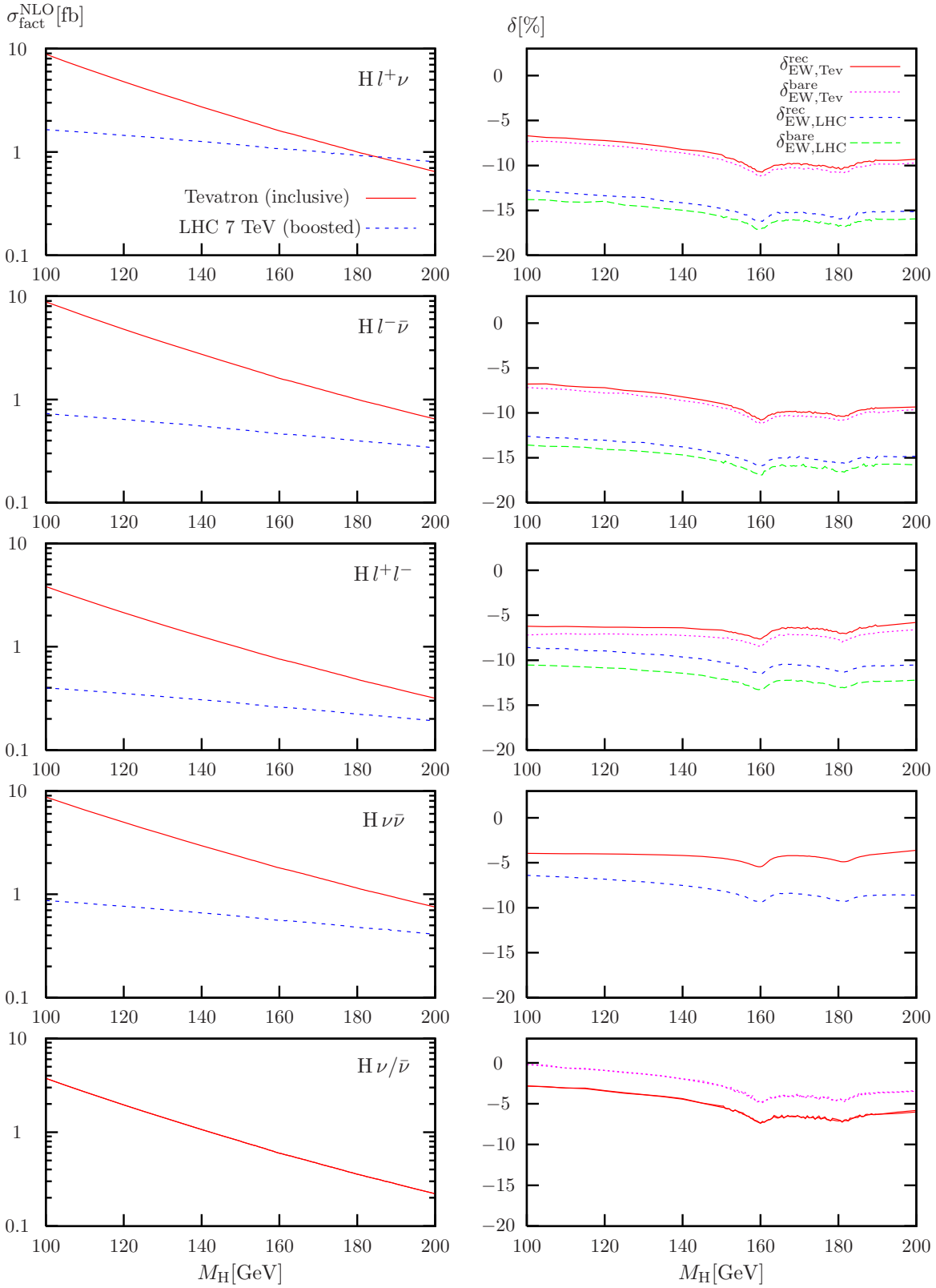

Figure 4: The cross section $\sigma^{\rm NLO}_{\rm fact}$ (left) and NLO EW corrections (right) for the different Higgs-strahlung processes with basic cuts at the Tevatron as well as for boosted Higgs bosons at the 7 TeV LHC as a function of the Higgs-boson mass.

channel	$\mathrm{H}l^+\nu_l + X$	$\mathrm{H}l^-\bar{\nu}_l + X$	$\mathrm{H}l^+l^- + X$	$\mathrm{H}\nu_l\bar{\nu}_l + X$	$\mathrm{H}\nu_l/\bar{\nu}_l + X$
σ_0/ fb	4.1232(2)	4.1229(2)	1.82773(5)	4.1480(1)	1.6063(2)
σ^{LO}/ fb	3.6930(5)	3.6926(5)	1.6484(1)	3.7476(4)	1.4355(4)
$\delta_{\mathrm{EW}}^{\mathrm{bare}}/\%$	-7.8	-7.8	-7.2	-4.1	-0.9
$\delta_{\mathrm{EW}}^{\mathrm{rec}}/\%$	-7.3	-7.3	-6.3	-4.1	-3.5
$\delta_{\mathrm{QCD}}/\%$	$+24.9$	$+24.9$	$+24.6$	$+24.9$	$+25.1$
$(K_{\mathrm{QCD}}-1)/\%$	$+39.5$	$+39.5$	$+38.1$	$+38.2$	$+40.0$
$\delta_\gamma/\%$	$+0.3$	$+0.3$	$+0.0$	-0.0	$+1.0$
$\sigma_{\mathrm{fact}}^{\mathrm{NLO}}$/ fb	4.7884(5)	4.7872(5)	2.1332(1)	4.9696(3)	1.9566(4)
$\sigma_{\mathrm{HAWK}}^{\mathrm{NLO}}$/ fb	4.8635(5)	4.8622(5)	2.1616(1)	5.0115(3)	1.9706(4)

Table 1: Born cross sections σ_0 and σ^{LO} evaluated with NLO and LO PDFs, respectively, various relative corrections, and the resulting predictions for inclusive production in the various Higgs-strahlung processes ($M_{\mathrm{H}} = 120\,\mathrm{GeV}$, Tevatron) according to (3.8) and (3.9). All relative corrections δ are given relative to σ_0, and $K_{\mathrm{QCD}} = \sigma_{\mathrm{QCD}}^{\mathrm{NLO}}/\sigma^{\mathrm{LO}}$.

channel	$\mathrm{H}l^+\nu_l + X$	$\mathrm{H}l^-\bar{\nu}_l + X$	$\mathrm{H}l^+l^- + X$	$\mathrm{H}\nu_l\bar{\nu}_l + X$	$\mathrm{H}\nu_l/\bar{\nu}_l + X$
σ_0/ fb	1.50846(7)	0.66292(3)	0.35349(2)	0.74759(3)	0.058236(9)
σ^{LO}/ fb	1.4183(2)	0.60926(9)	0.32845(5)	0.69519(9)	0.05417(3)
$\delta_{\mathrm{EW}}^{\mathrm{bare}}/\%$	-14.2	-14.0	-10.9	-6.9	-12.5
$\delta_{\mathrm{EW}}^{\mathrm{rec}}/\%$	-13.3	-13.0	-9.0	-6.9	-14.5
$\delta_{\mathrm{QCD}}/\%$	$+9.5$	$+9.4$	$+9.8$	$+9.8$	$+6.8$
$(K_{\mathrm{QCD}}-1)/\%$	$+16.5$	$+19.1$	$+18.1$	$+18.1$	$+14.9$
$\delta_\gamma/\%$	$+1.3$	$+1.5$	$+0.0$	$+0.0$	$+12.5$
$\sigma_{\mathrm{fact}}^{\mathrm{NLO}}$/ fb	1.4522(4)	0.6406(2)	0.35329(7)	0.7646(2)	0.06043(6)
$\sigma_{\mathrm{HAWK}}^{\mathrm{NLO}}$/ fb	1.4713(4)	0.6488(2)	0.35639(7)	0.7697(2)	0.06100(6)

Table 2: Born cross sections, various corrections, and the resulting predictions for boosted production in the various Higgs-strahlung processes ($M_{\mathrm{H}} = 120\,\mathrm{GeV}$, LHC at 7 TeV). See Table 1 for details.

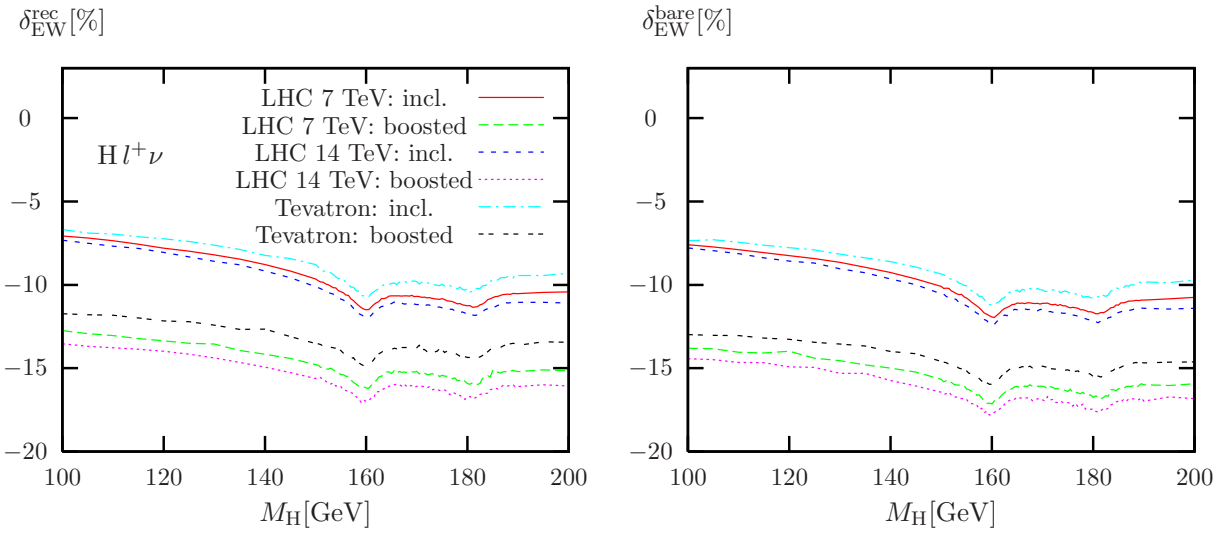

Figure 5: EW corrections with (left) and without (right) lepton–photon recombination for H$l^+\nu_l$ production at the LHC at 7 TeV and at 14 TeV and at the Tevatron as a function of the Higgs-boson mass.

Figure 7 shows the differential cross sections with respect to the transverse momentum of the Higgs boson up to 300 GeV, along with the EW corrections. For the inclusive Higgs-boson sample, the EW corrections range between −5% and −15% and are largest for the W-mediated channels at large $p_{\rm T,H}$. The difference due to the treatment of final-state photons is again small, since the bulk of the correction is of weak origin and not due to final-state radiation. The same observation holds for large values of the transverse momentum in the boosted-Higgs analysis. However, close to the cut value of 200 GeV for $p_{\rm T,H}$, the corrections receive a sizeable negative contribution from final-state radiation effects, in particular for the Hl^+l^- channel, since we also require $p_{{\rm T},V} > 190$ GeV. Final-state radiation can destroy the perfect balance between the Higgs- and the vector-boson transverse momentum at Born level. This balance is also influenced by initial-state radiation and would lead to a breakdown of the fixed-order calculation near the cut if the cuts on $p_{\rm T,H}$ and $p_{\rm T,W/Z}$ were equal. As mentioned above, the photon-induced contributions are large for the H$\nu_l/\overline{\nu}_l$ channel in the boosted analysis, but the overall contribution is small and phenomenologically unimportant.

Figure 8 shows the differential cross section with respect to the transverse momentum of the vector boson, i.e. the sum of the transverse momenta of the leptons in the final state (or the transverse momentum of the neutrino in the H$\nu_l/\overline{\nu}_l$ case, as discussed at the end of Section 2). The EW corrections are very similar to the ones for the $p_{\rm T,H}$ distribution. Only the large contribution due to final-state radiation near the cut in the boosted analysis is absent because the Higgs boson is uncharged (possible final-state radiation of the Higgs decay products is not available in our analysis). However, near $p_{\rm T,W/Z} = 200$ GeV the perturbative uncertainty due to QCD initial-state radiation rises, since there is no tree-level distribution below the value of the $p_{\rm T,H}$ cut. In Figure 8, one observes a sharp drop of the cross section in the first bin of the distribution which is due to correspondingly large NLO QCD corrections.

The differential distributions with respect to the rapidity of the Higgs boson and the transverse momentum of a positively charged lepton in the final state are displayed in Figures 9 and 10, respectively. The EW corrections for the rapidity distribution are almost completely flat and, hence, resemble the correction for the cross section using a given set of cuts. The transverse-

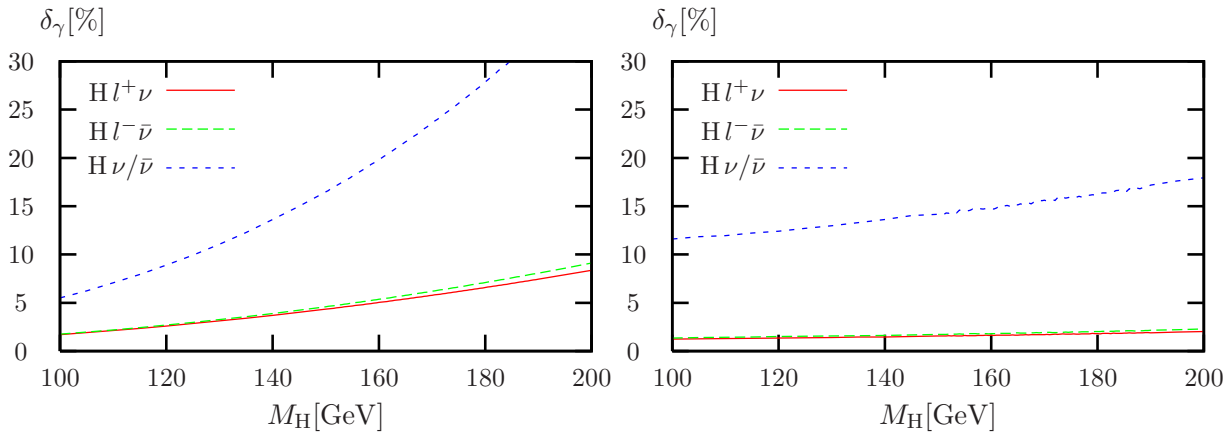

Figure 6: Relative correction from photon-induced processes for basic cuts (left) and the boosted-Higgs analysis (right) at the 7 TeV LHC as a function of the Higgs-boson mass.

momentum distribution shows corrections growing in absolute size with the energy of the typical events as observed before, close to or even beyond -20% at $p_{\mathrm{T},l^+} = 300\,\mathrm{GeV}$ with recombination or for bare muons, respectively.

Finally, Figure 11 shows that for the $\mathrm{H}l^+\nu_l$ channel the EW corrections hardly differ for the same observable measured at different hadron colliders. Only the photon-induced corrections are more sensitive to the specific collider settings. Exemplarily, the distribution with respect to the transverse momentum of the Higgs boson is shown but other distributions show the same qualitative behaviour.

4 Conclusions

In this paper we have discussed the impact of electroweak radiative corrections to the Higgs-strahlung processes off W/Z bosons, $\mathrm{pp/p\bar{p}} \to \mathrm{H}l\nu_l/l^-l^+/\nu_l\bar{\nu}_l + X$, at the Tevatron and the LHC. Compared to a previous calculation, we provide fully differential predictions. We include the leptonic decays of the W and Z bosons and support the full kinematical information on the Higgs boson and the decay leptons of the weak gauge bosons. These processes and the corresponding next-to-leading-order QCD and electroweak corrections are included in the new version 2.0 of the Monte Carlo program HAWK, which was initially designed for Higgs + 2 jet production via vector-boson fusion and WH/ZH production with hadronically decaying W/Z bosons.

The electroweak corrections are of the order of $-(5{-}10)\%$ for total cross sections and, thus, larger than the uncertainty originating from parton distribution functions and QCD factorization and renormalization scales. Our detailed discussion of the electroweak corrections to transverse-momentum and rapidity distributions of the Higgs boson and outgoing charged leptons demonstrates that the corrections further increase in size in the regions of increasing transverse momenta. For instance, imposing the cut $p_{\mathrm{T,H}} > 200\,\mathrm{GeV}$ at the LHC, which is part of the search strategy for highly-boosted Higgs bosons decaying into "fat jets" with $\mathrm{b\bar{b}}$ substructure, drives the corrections to WH production to about -14% for $M_{\mathrm{H}} = 120\,\mathrm{GeV}$. The electroweak corrections to the different p_{T} distributions can already exceed -15% in the range $p_{\mathrm{T}} = 200{-}300\,\mathrm{GeV}$ and grow further when more energetic events are analyzed.

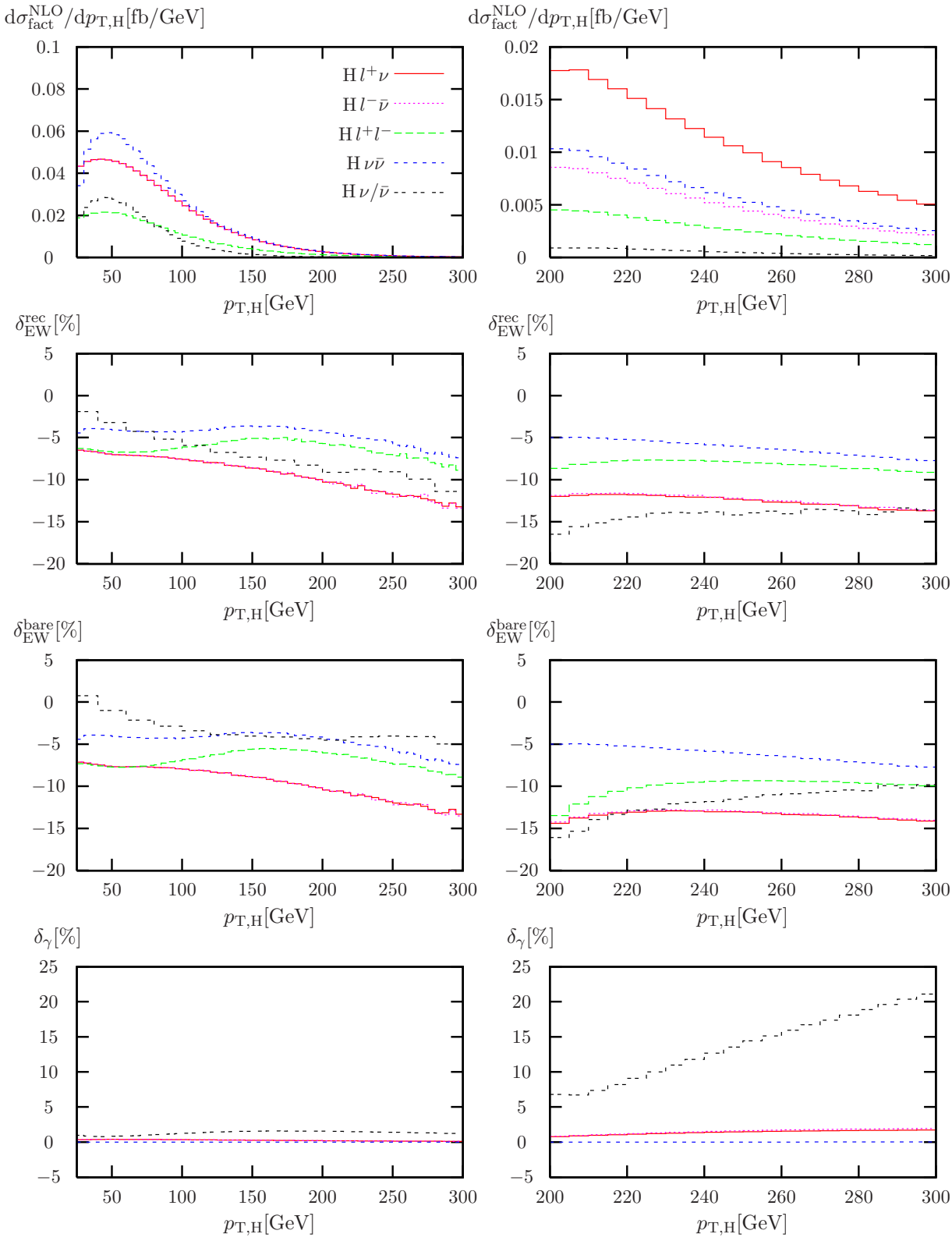

Figure 7: The $p_{T,H}$ distributions $d\sigma^{NLO}_{fact}/dp_{T,H}$ (top), NLO EW corrections for recombined and bare leptons (middle), and corrections due to photon-induced processes (bottom) for Higgs-strahlung with basic cuts at the Tevatron (left) as well as for boosted Higgs bosons at the 7 TeV LHC (right) for $M_H = 120\,\text{GeV}$.

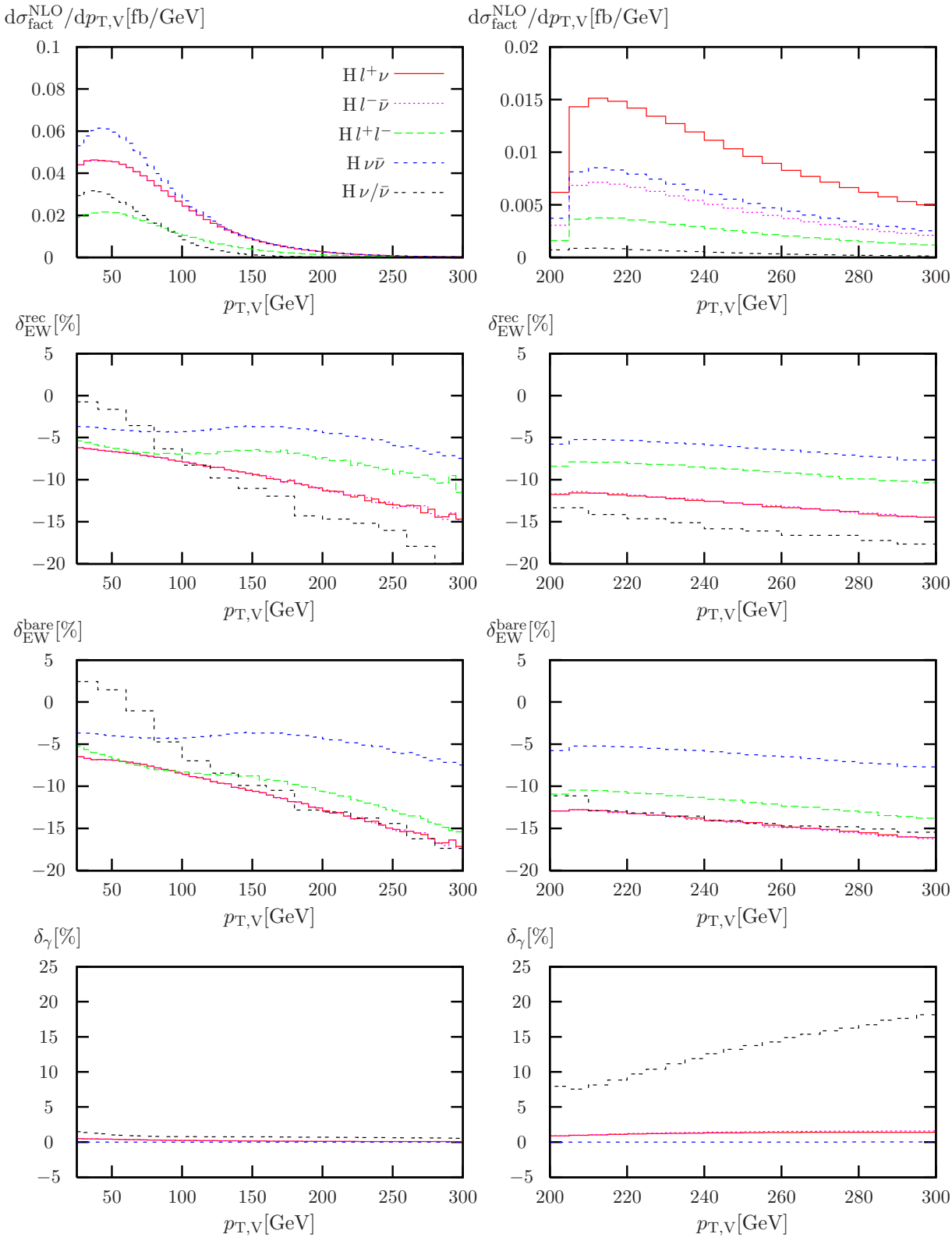

Figure 8: The $p_{T,V}$ distributions $d\sigma^{NLO}_{fact}/dp_{T,V}$ (top), NLO EW corrections for recombined and bare leptons (middle), and corrections due to photon-induced processes (bottom) for Higgs-strahlung with basic cuts at the Tevatron (left) as well as for boosted Higgs bosons at the 7 TeV LHC (right) for $M_H = 120\,\text{GeV}$.

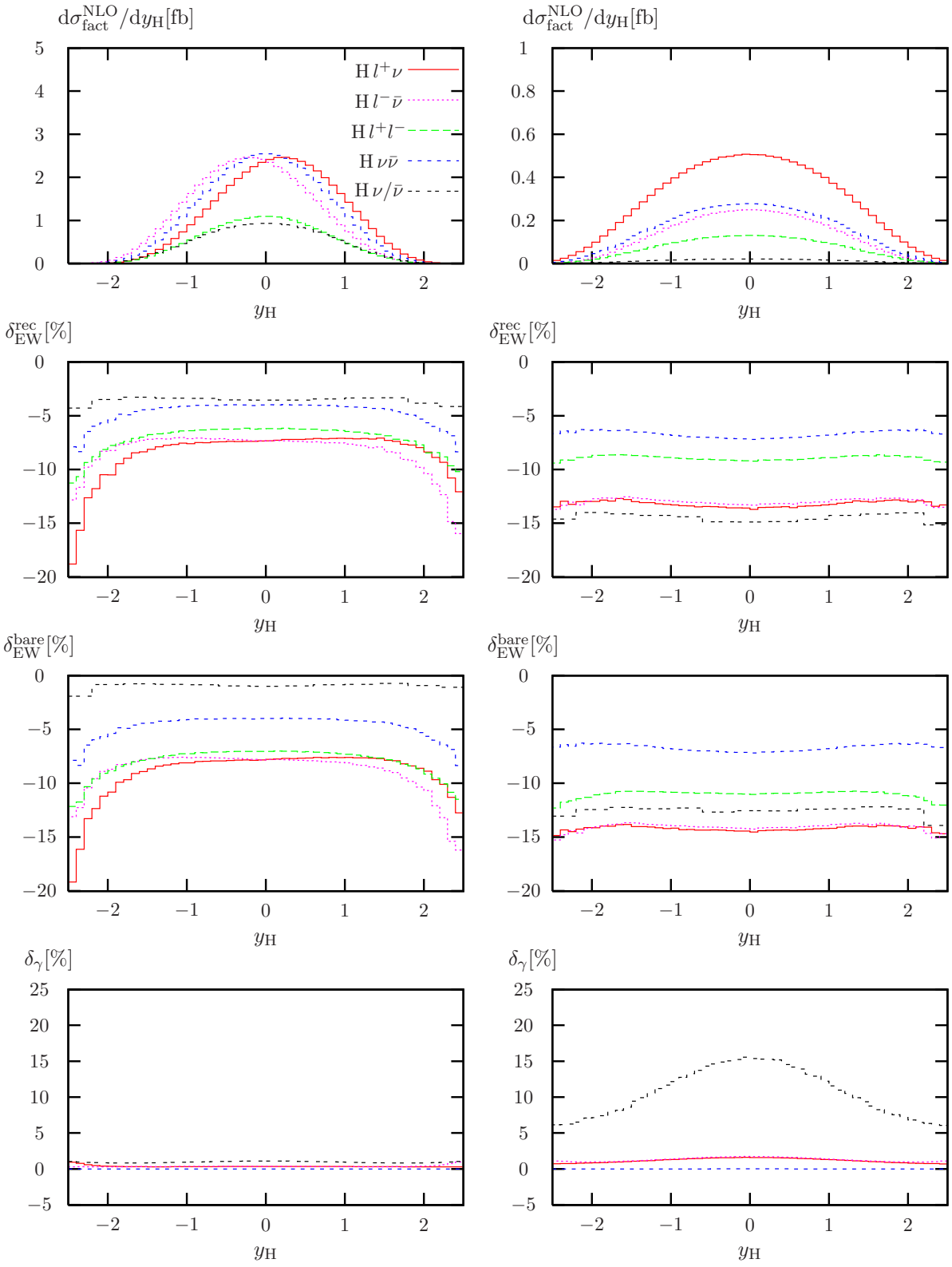

Figure 9: The y_H distributions $d\sigma^{NLO}_{fact}/dy_H$ (top), NLO EW corrections for recombined and bare leptons (middle), and corrections due to photon-induced processes (bottom) for Higgs-strahlung with basic cuts at the Tevatron (left) as well as for boosted Higgs bosons at the 7 TeV LHC (right) for $M_H = 120$ GeV.

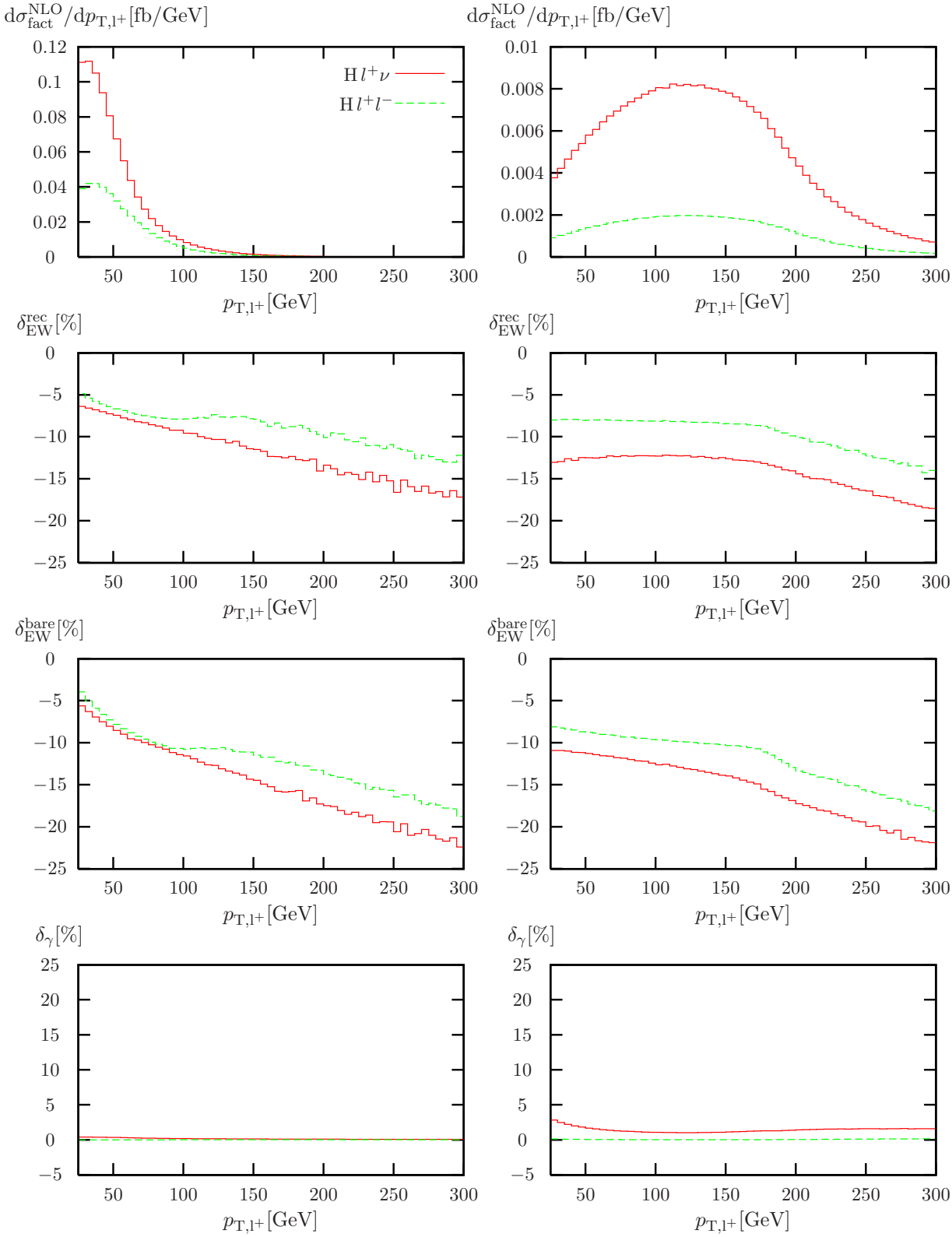

Figure 10: The p_{T,l^+} distributions $d\sigma^{NLO}_{fact}/dp_{T,l^+}$ (top), NLO EW corrections for recombined and bare leptons (middle), and corrections due to photon-induced processes (bottom) for Higgs-strahlung with basic cuts at the Tevatron (left) as well as for boosted Higgs bosons at the 7 TeV LHC (right) for $M_H = 120\,\text{GeV}$.

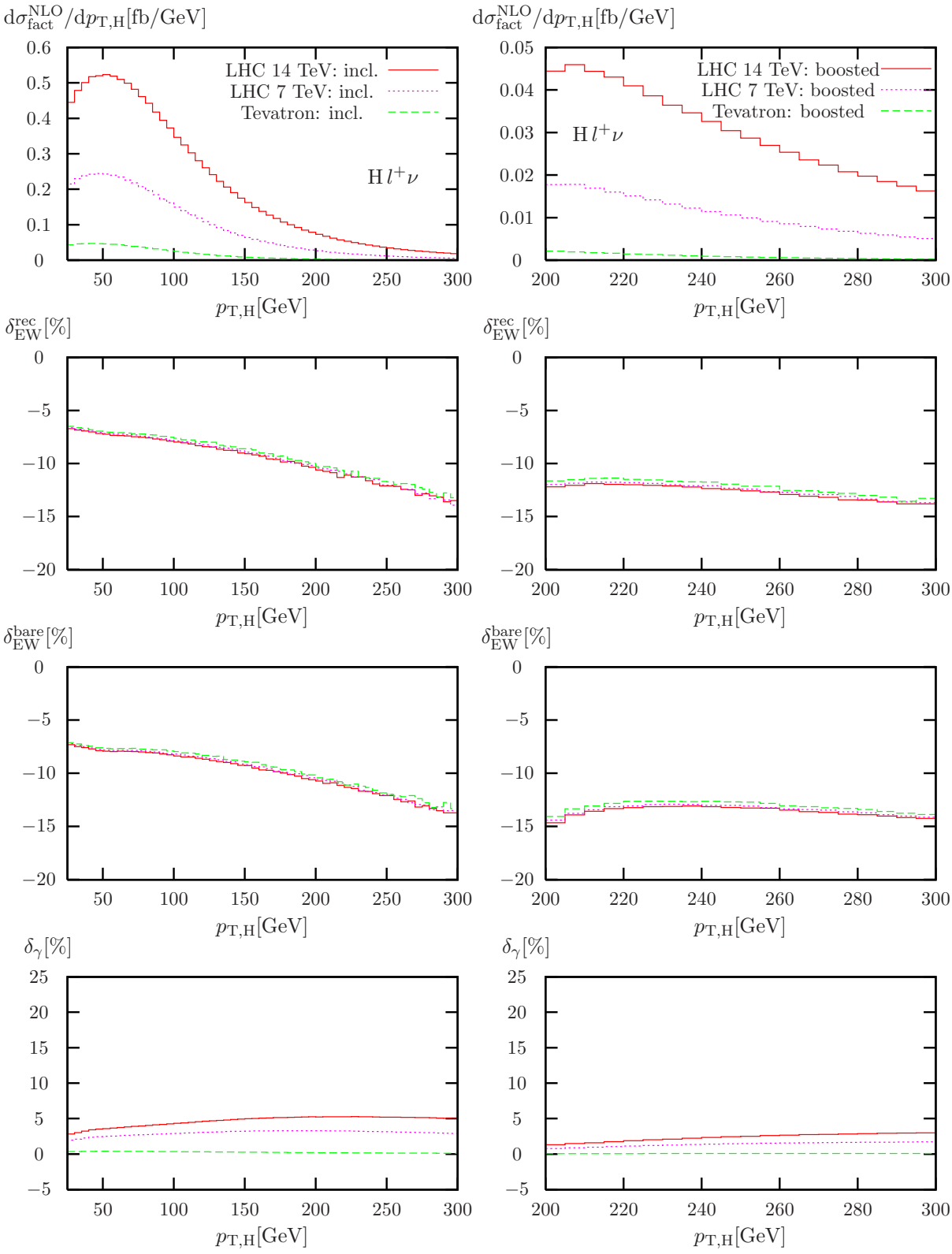

Figure 11: The $p_{T,H}$ distributions $d\sigma^{NLO}_{fact}/dp_{T,H}$ (top), NLO EW corrections for recombined and bare leptons (middle) and corrections due to photon-induced processes (bottom) for for $Hl^+\nu_l$ production and different collider setups with basic cuts (left) and additional cuts for boosted-Higgs analyses (right) for $M_H = 120\,\text{GeV}$.

Electroweak corrections, thus, represent an important ingredient in the theory predictions for Higgs-strahlung off W/Z bosons at the Tevatron and the LHC.

Acknowledgements

This work is supported in part by the Gottfried Wilhelm Leibniz programme of the Deutsche Forschungsgemeinschaft (DFG). We thank the members of the LHC Higgs Cross Section Working Group, in particular J. Olsen and G. Piacquadio for useful discussions on the experimental setup.

References

[1] The ATLAS collaboration, ATLAS-CONF-2011-163;
The CMS collaboration, CMS-PAS-HIG-11-032.

[2] J. M. Butterworth, A. R. Davison, M. Rubin, G. P. Salam, Phys. Rev. Lett. **100** (2008) 242001 [arXiv:0802.2470 [hep-ph]];
J. M. Butterworth *et al.*, ATL-PHYS-PUB-2009-088.

[3] T. Han, S. Willenbrock, Phys. Lett. **B273** (1991) 167;
H. Baer, B. Bailey, J. F. Owens, Phys. Rev. **D47** (1993) 2730;
J. Ohnemus, W. J. Stirling, Phys. Rev. **D47** (1993) 2722.

[4] M. Spira, V2HV, http://people.web.psi.ch/spira/v2hv, 2007.

[5] J. Campbell, K. Ellis, MCFM – Monte Carlo for FeMtobarn processes, http://mcfm.fnal.gov, 2010.

[6] O. Brein, A. Djouadi, R. Harlander, Phys. Lett. **B579** (2004) 149 [hep-ph/0307206].

[7] R. Hamberg, W. L. van Neerven, T. Matsuura, Nucl. Phys. **B359** (1991) 343.

[8] O. Brein, R. Harlander, M. Wiesemann, T. Zirke, arXiv:1111.0761 [hep-ph].

[9] M. L. Ciccolini, S. Dittmaier, M. Krämer, Phys. Rev. **D68** (2003) 073003 [hep-ph/0306234].

[10] O. Brein *et al.*, hep-ph/0402003.

[11] S. Dittmaier *et al.* [LHC Higgs Cross Section Working Group Collaboration], CERN-2011-002, arXiv:1101.0593 [hep-ph].

[12] G. Ferrera, M. Grazzini, F. Tramontano, arXiv:1107.1164 [hep-ph].

[13] A. Denner, S. Dittmaier, M. Roth, D. Wackeroth, Nucl. Phys. B **560** (1999) 33 [hep-ph/9904472].

[14] A. Denner, S. Dittmaier, M. Roth and L. H. Wieders, Nucl. Phys. B **724** (2005) 247 [Erratum-ibid. B **854** (2012) 504] [hep-ph/0505042].

[15] M. Ciccolini, A. Denner, S. Dittmaier, Phys. Rev. Lett. **99** (2007) 161803 [arXiv:0707.0381 [hep-ph]] and Phys. Rev. **D77** (2008) 013002 [arXiv:0710.4749 [hep-ph]].

[16] A. Denner, S. Dittmaier, S. Kallweit, A. Mück, HAWK, http://omnibus.uni-freiburg.de/sd565/programs/hawk/hawk.html, 2010.

[17] T. Hahn, Comput. Phys. Commun. **140** (2001) 418 [hep-ph/0012260];
T. Hahn, C. Schappacher, Comput. Phys. Commun. **143** (2002) 54 [hep-ph/0105349].

[18] T. Hahn, M. Pérez-Victoria, Comput. Phys. Commun. **118** (1999) 153 [hep-ph/9807565].

[19] S. Dittmaier, Phys. Rev. D **59** (1999) 016007 [hep-ph/9805445].

[20] E. Accomando, A. Denner, C. Meier, Eur. Phys. J. C **47** (2006) 125 [hep-ph/0509234].

[21] S. Dittmaier, M. Roth, Nucl. Phys. B **642** (2002) 307 [hep-ph/0206070].

[22] A. Bredenstein, A. Denner, S. Dittmaier, M. M. Weber, Phys. Rev. **D74** (2006) 013004 [hep-ph/0604011] and JHEP **0702** (2007) 080 [hep-ph/0611234].

[23] A. Denner, Fortsch. Phys. **41** (1993) 307 [arXiv:0709.1075 [hep-ph]].

[24] A. Denner, G. Weiglein, S. Dittmaier, Nucl. Phys. B **440** (1995) 95 [hep-ph/9410338].

[25] J. Küblbeck, M. Böhm, A. Denner, Comput. Phys. Commun. **60** (1990) 165;
H. Eck, J. Küblbeck, *Guide to FeynArts 1.0*, University of Würzburg, 1992.

[26] A. Denner, S. Dittmaier, Nucl. Phys. B **658** (2003) 175 [hep-ph/0212259].

[27] A. Denner, S. Dittmaier, Nucl. Phys. B **734** (2006) 62 [hep-ph/0509141].

[28] G. Passarino, M. Veltman, Nucl. Phys. B **160** (1979) 151.

[29] A. Denner, S. Dittmaier, Nucl. Phys. **B844** (2011) 199 [arXiv:1005.2076 [hep-ph]].

[30] S. Catani, M. H. Seymour, Nucl. Phys. B **485** (1997) 291 [Erratum-ibid. B **510** (1998) 503] [hep-ph/9605323].

[31] S. Dittmaier, Nucl. Phys. B **565** (2000) 69 [hep-ph/9904440].

[32] S. Dittmaier, A. Kabelschacht, T. Kasprzik, Nucl. Phys. B **800** (2008) 146 [arXiv:0802.1405 [hep-ph]].

[33] A. D. Martin, R. G. Roberts, W. J. Stirling, R. S. Thorne, Eur. Phys. J. C **39** (2005) 155 [hep-ph/0411040].

[34] H. Spiesberger, Phys. Rev. D **52** (1995) 4936 [hep-ph/9412286];
M. Roth, S. Weinzierl, Phys. Lett. **B590** (2004) 190 [hep-ph/0403200].

[35] T. Kinoshita, J. Math. Phys. **3** (1962) 650;
T. D. Lee, M. Nauenberg, Phys. Rev. **133** (1964) B1549.

[36] C. Amsler *et al.* [Particle Data Group], Phys. Lett. B **667** (2008) 1.

[37] D. Y. Bardin, A. Leike, T. Riemann, M. Sachwitz, Phys. Lett. B **206** (1988) 539.

[38] A. D. Martin *et al.*, Eur. Phys. J. **C63**, (2009) 189 [arXiv:0901.0002 [hep-ph]].

[39] M. R. Whalley, D. Bourilkov, R. C. Group, in *HERA and the LHC*, eds. A. de Roeck, H. Jung (CERN-2005-014, Geneva, 2005), p. 575, hep-ph/0508110.

[40] S. Dittmaier *et al.* [LHC Higgs Cross Section Working Group Collaboration], in preparation.

[41] private communication with J. Olson, G. Piacquadio within the WH/ZH subgroup of the LHC Higgs Cross Section Working Group Collaboration.